JOURNAL OF MATERIALS SCIENCE **40** (2005) 5215–5221

Microscopic and macroscopic magnetic properties of $MgAl_xCr_xFe_{2-2x}O_4$ spinel ferrite system

K. P. THUMMER, M. P. PANDYA, K. H. JANI, K. B. MODI, H. H. JOSHI
Department of Physics, Saurashtra University, Rajkot-360 005, India

In order to study the effect of co-substitution of Al^{3+} and Cr^{3+} for Fe^{3+} in $MgFe_2O_4$ on its structural and magnetic properties, the spinel system $MgAl_xCr_xFe_{2-2x}O_4$ ($x = 0.0$–0.8) has been characterized by X-ray diffraction, high field magnetization, low field a.c. susceptibility and ^{57}Fe Mössbauer spectroscopy measurements. Contrary to the earlier reports, about 50% of Al^{3+} is found to occupy the tetrahedral sites. The system exhibits canted spin structure and a central paramagnetic doublet was found superimposed on the magnetic sextet in the Mössbauer spectra ($0.5 > x > 0.2$). Thermal variation of a.c. susceptibility exhibits normal ferrimagnetic behaviour.

1. Introduction

The system under investigation, $MgAl_xCr_xFe_{2-2x}O_4$, consists of magnesium ferrite aluminate ($MgAl_xFe_{2-x}O_4$) and magnesium ferrite chromate ($MgCr_xFe_{2-x}O_4$) in equal proportions, which can be prepared by co-substituting Al^{3+} (diamagnetic; 0 μ_B) and Cr^{3+}/(magnetic; 3 μ_B) ions for Fe^{3+} (magnetic; 5 μ_B) ions in $MgFe_2O_4$. According to the literature [1, 2] $MgFe_2O_4$ ($x = 0.0$) is a partially inverse spinel and it can be considered as a collinear ferrimagnet whose degree of inversion depends upon the thermal history of the sample. $MgCr_2O_4$ is a normal spinel with canted ferrimagnetic structure [3]. $MgAl_2O_4$ (mineral spinel) is a partially inverted spinel in which the ratio of Al^{3+} ions in the tetrahedral (A) and octahedral (B) sites [4] is about 1:6 [4].

No systematic investigations of the crystal structure, cation distributions and magnetic properties of $MgAl_xCr_xFe_{2-2x}O_4$ for $x = 0.0$–0.8 have been reported in the literature. Though structural and magnetic properties of $MgAl_xFe_{2-x}O_4$ [5–7] and $MgCr_xFe_{2-x}O_4$ [3, 8] have been studied separately, no attempt has been made to study the combined effect of Al-Cr substitution for Fe in $MgFe_2O_4$. Recently, it has been reported that when spinel ferrites or garnets are co-substituted by Al^{3+} and Cr^{3+} the magnetic properties are modified and show interesting behaviour [9–14]. The purpose of this paper is to present the results of a systematic investigation of the crystal structure, cation distribution, and magnetic properties of $MgAl_xCr_xFe_{2-2x}O_4$ ($x = 0.0$–0.8) mixed spinels by means of X-ray diffraction, magnetization, a.c.susceptibility and Mössbauer spectroscopic measurements.

2. Experimental details

The polycrystalline powders of the spinel solid solution series $MgAl_xCr_xFe_{2-2x}O_4$ were prepared by usual double sintering ceramic technique for $x = 0.0$–0.8, step 0.1. The oxides of the metal ions were used as starting materials. The materials used were of AR grade with 99.9% purity. The starting materials procured from E. Merck, were taken in the required proportions and mixed. The mixed powder was ground, pelletized and pre-sintered at 950°C in air for 24 h. In the final sintering process, the samples were placed in furnace at 1100°C for 24 h in air and then slowly cooled to room temperature at the rate of 2°C/min.

The X-ray diffraction patterns of all the samples were recorded at 300 K with a Philips (PM 9220) diffractometer using Cu K_α adiation. The stoichiometry of the powdered samples was checked by energy dispersive X-ray analysis (EDAX). No traces of any impurities were found. Magnetization measurements on each sample were carried out using the high field hysteresis loop technique [15] at 300 and 77 K. The a.c.susceptibility measurements on powdered samples were made in the temperature range 300–700 K using a double coil set-up [16] operating at a frequency of 263 Hz in an rms field of 0.5 Oe.

The Mössbauer spectra were obtained with a constant acceleration transducer and a 256 multichannel analyzer operating in time mode. A gamma source of ^{57}Co (Pd) of 5 mCi was used. All the spectra were obtained at 300 K in transmission geometry and the 14.4 keV gamma rays were detected with a Xenon-methane filled proportional counter.

3. Results and discussion

The X-ray diffraction patterns of all the samples show sharp lines which make detection of any impurity phase easy and enable the accurate determination of lattice constant. It is clear from the indexed X-ray diffraction patterns that all the samples are single phase fcc spinels. No traces of any impurity were found.

0022–2461
DOI: 10.1007/s10853-005-4415-0

The lattice constant 'a' for each composition was determined accurately using the Nelson-Riley method [17].

In order to determine the cation distributions, X-ray intensity calculations were made using the formula suggested by Buerger [18]. The intensity ratios of the planes considered to be sensitive to the cation distribution parameter (x) were taken for estimating the cation distributions. The ionic configuration based on site preference energies values for individual cations in $MgAl_xCr_xFe_{2-2x}O_4$ suggests that Cr^{3+} ion has marked preference for octahedral (B-) sites while Mg^{2+}, Al^{3+} and Fe^{3+} ions can occupy both A- and B-sites. There is a good contrast in the atomic scattering factor of Fe^{3+} and other cations present in the system. This makes the determination of cations distribution quite reliable. Moreover, any alteration in the distribution of cations causes significant changes in the theoretical values of X-ray diffraction intensity ratios.

Therefore, in the process of arriving at the final cation distribution, the site occupancy of all the cations was varied for many combinations. The final cation distributions deduced by simultaneously considering the Bragg plane ratios and the fitting of the magnetization data at 77 K are as follows:

$$
\begin{aligned}
x = 0.0 &\quad \left(Mg^{+2}_{0.13}Fe^{+3}_{0.87}\right)^{A} \quad \left[Mg^{+2}_{0.87}Fe^{+3}_{1.13}\right]^{B} O^{-2}_{4}\\
x = 0.1 &\quad \left(Mg^{+2}_{0.13}Al^{+3}_{0.1}Fe^{+3}_{0.77}\right)^{A} \quad \left[Mg^{+2}_{0.87}Cr^{+3}_{0.1}Fe^{+3}_{1.03}\right]^{B} O^{-2}_{4}\\
x = 0.2 &\quad \left(Mg^{+2}_{0.13}Al^{+3}_{0.2}Fe^{+3}_{0.67}\right)^{A} \quad \left[Mg^{+2}_{0.87}Cr^{+3}_{0.2}Fe^{+3}_{0.93}\right]^{B} O^{-2}_{4}\\
x = 0.3 &\quad \left(Mg^{+2}_{0.13}Al^{+3}_{0.25}Fe^{+3}_{0.62}\right)^{A} \quad \left[Mg^{+2}_{0.87}Cr^{+3}_{0.3}Fe^{+3}_{0.78}Al^{+3}_{0.03}\right]^{B} O^{-2}_{4}\\
x = 0.4 &\quad \left(Mg^{+2}_{0.13}Al^{+3}_{0.3}Fe^{+3}_{0.57}\right)^{A} \quad \left[Mg^{+2}_{0.87}Cr^{+3}_{0.4}Fe^{+3}_{0.63}Al^{+3}_{0.1}\right]^{B} O^{-2}_{4}\\
x = 0.5 &\quad \left(Mg^{+2}_{0.13}Al^{+3}_{0.35}Fe^{+3}_{0.52}\right)^{A} \quad \left[Mg^{+2}_{0.87}Cr^{+3}_{0.5}Fe^{+3}_{0.48}Al^{+3}_{0.15}\right]^{B} O^{-2}_{4}\\
x = 0.6 &\quad \left(Mg^{+2}_{0.13}Al^{+3}_{0.4}Fe^{+3}_{0.47}\right)^{A} \quad \left[Mg^{+2}_{0.87}Cr^{+3}_{0.6}Fe^{+3}_{0.33}Al^{+3}_{0.2}\right]^{B} O^{-2}_{4}\\
x = 0.7 &\quad \left(Mg^{+2}_{0.13}Al^{+3}_{0.45}Fe^{+3}_{0.42}\right)^{A} \quad \left[Mg^{+2}_{0.87}Cr^{+3}_{0.7}Fe^{+3}_{0.18}Al^{+3}_{0.25}\right]^{B} O^{-2}_{4}\\
x = 0.8 &\quad \left(Mg^{+2}_{0.13}Al^{+3}_{0.5}Fe^{+3}_{0.37}\right)^{A} \quad \left[Mg^{+2}_{0.87}Cr^{+3}_{0.8}Fe^{+3}_{0.03}Al^{+3}_{0.3}\right]^{B} O^{-2}_{4}
\end{aligned}
\qquad (1)
$$

The variation of the lattice constant as a function of Al-Cr content (x) is depicted in Fig. 1, which exhibits a slower rate of decrease up to $x = 0.4$ and thereafter it decreases with faster rate. The overall decrease in the lattice constant is apparent because the larger cation Fe^{3+} (0.64 Å) is replaced by the smaller ones; Cr^{3+} (0.63 Å) and Al^{3+} (0.51 Å) in the system. The linear variation of lattice constant indicates that the system obeys Vegard's law [19]. The initial rate of decrease of 'a' is slow because the smaller cation Al^{3+} prefers to occupy the tetrahedral sites and replaces the larger cations Fe^{3+} to the octahedral site: (Equation 1). The inter-play of Al^{3+} and Fe^{3+} cations causes the different rate of decrease of lattice constant in the system. It is clear from (Equation 1) that up to $x = 0.4$, a maximum of 25% of Al^{3+} ions occupies the octahedral sites, thereafter, the octahedral site occupancy increases up to 38% in case of composition $x = 0.6$. The initial ferrite $MgFe_2O_4$ ($x = 0.0$) shows a degree of inversion 0.87 and it remains constant throughout the series. Contrary to reports [6, 20–22] that Al^{3+} ions show a preference for octahedral sites, we have found by means of the X-ray diffraction analysis that a larger fraction of Al^{3+} enters into tetrahedral sites. The atomic scattering factors for Mg^{2+} and Al^{3+} [17] are same but the scattering factor of Fe^{3+} is about three times that of Al^{3+} and Mg^{2+}, which renders good contrast between Fe^{3+} and Al^{3+}. Therefore, the distribution of Al^{3+} and Fe^{3+} can be accurately determined. The cation distributions determined through X-ray diffraction are compared with the results obtained from magnetization (at 77 K) and from Mössbauer spectroscopy. The X-ray density decreases linearly (Fig. 1) with Al-Cr content (x) in spite of the decrease in unit cell volume suggesting that the decrease in mass overtakes the decrease in unit cell volume.

The variation of magnetization as a function of the applied magnetic field (M versus H curves) recorded at 300 K (Fig. 2) exhibits a 'high field slope' (i.e., non-saturating behaviour) for the samples with $x \geq 0.3$ indicating non-collinear spin structure. The values of saturation magnetization (σ_s) at 77 and 300 K are listed in Table I. It is observed that σ_s initially increases

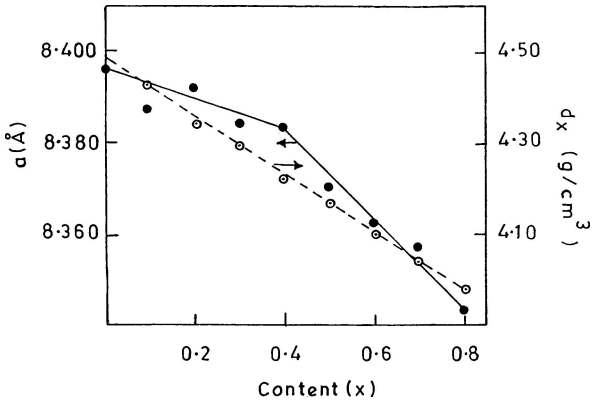

Figure 1 Variation of lattice constant, a (Å) and X-ray density (d_x) as a function of Al-Cr content (x).

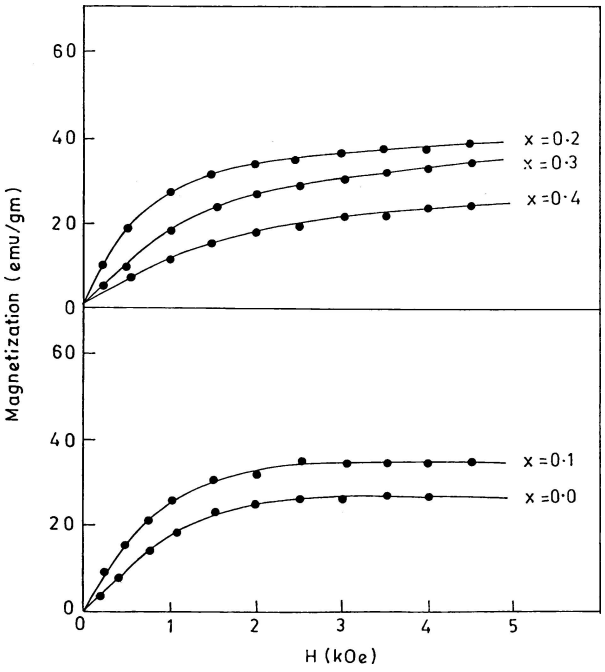

Figure 2 Field dependence of magnetization at 300 K.

TABLE I Saturation magnetization (σ_s) and magneton number (n_B) for $MgAl_xCr_xFe_{2-2x}O_4$ system

	300 K		77 K			
Content (x)	σ_s (emu/gm)	n_B (μ_B)	σ_s (emu/gm)	n_B (μ_B)	N n_B (μ_B)	n_B* (μ_B)
0.0	27	0.97	36	1.30	1.30	1.30
0.1	34	1.20	45	1.60	1.60	1.60
0.2	38	1.32	55	1.90	1.90	1.90
0.3	35	1.19	48	1.53	1.71	1.53
0.4	25	0.82	43	1.30	1.53	1.30
0.5	10	0.32	37	1.08	1.30	1.09
0.6	–	–	25	0.81	1.11	0.82
0.7	–	–	17	0.52	0.75	0.53
0.8	–	–	09	0.27	–	–

up to $x = 0.2$; thereafter it decreases with increasing Al-Cr concentration. The variation of the magneton number (n_B) with x can be explained by invoking Neel's collinear or 'canted' spin structure. The canted spin structure is stable at lower temperatures and it disappears on approaching the Neel temperature (T_N). The canting angles can be related to the magnetic dilution by using non-collinear spin models based on molecular field theory.

Since the values of T/T_N at $T = 300$ K are greater than 0.55 for the system $MgAl_xCr_xFe_{2-2x}O_4$, it is not possible to investigate the 'spin structure' using the room-temperature (300 K) magnetization data. Therefore, the magnetization data recorded at 77 K (where $T/T_N < 0.2$) (Table III) were used for the study of magnetic ordering in the present system.

According to the Neel's collinear spin configuration [22] the magnetic moment per formula unit in μ_B (n_B^N) is expressed as,

$$n_B^N = M_B(x) - M_A(x)$$

where, M_B and M_A are sublattice magnetizations calculated using the cation distribution (Equation 1) and the free ion magnetic moments of Fe^{3+} (5 μ_B) and Cr^{3+} (3 μ_B). It is clear from Table I that the n_B^N values agree with the observed n_B values at 77 K up to $x = 0.2$ but increasing discrepancies are observed with further magnetic dilution (x). This indicates a non-collinear spin structure for the samples with $x \geq 0.3$.

The magneton number at absolute zero (n_B^*) obtained by using the measured n_B at 77 K and the T/T_N values through the Brillouin function [23] ($j = 5/2$) are given in Table I There is a good agreement between n_B^N and n_B^* for the compositions $x \leq 0.2$ suggesting the magnetic structure to be collinear at these compositions. The discrepancy between n_B^N and n_B^* for the samples with the $x \geq 0.3$ indicates canted spin structure (Table I). The observation that $n_B^* < n_B^N$ for $x \geq 0.3$ is a clear symptom for the existence of a canted spin structure.

The initial composition i.e., $x = 0.0$; $MgFe_2O_4$ is a partially inverse spinel (degree of inversion = 0.87) and a collinear ferrimagnet. On Al^{3+} substitution the number of A-B superexchange interactions is reduced and the B-B interaction is made stronger because of the reduction in unit cell dimensions (Fig. 1) [24]. Both these factors induce a canted spin alignment in octahedral sites. It is apparent from the cation distributions that the major fraction of Al^{3+} ions prefers to occupy the A-sites, which replaces Fe^{3+} ions from A to B causing a reduction in A-B magnetic linkages. The observed variation of n_B as a function of Al-Cr concentration (x) is explained in terms of the Random Canting of Spin model [25]. It is more appropriate to use the RCS model instead of the Yafet-Kittel model as the actual canting at any site will depend not only on the number of diamagnetic nearest neighbours but also on their spatial arrangement.

The Mössbauer spectra recorded at 300 K for $x = 0.1$–0.5 are displayed in Figs 3 and 4. For the samples with $x = 0.0$–0.2, the spectra exhibit two normal Zeeman split sextets one due to the A-site Fe^{3+} ions and other due to B-site Fe^{3+} ions, which indicate ferrimagnetic behaviour of the samples. The solid lines through the data points in the Figs 3 and 4 are the results of computer fits of spectra obtained assuming equal line width for A- and B-sites. It is clear from Figs 3 and 4 that the spectrum for the compositions $x = 0.3$ and 0.4 exhibit a central paramagnetic doublet resulting from super paramagnetic Fe^{3+} species [26]. The Mössbauer spectrum of $x = 0.5$ shows features of relaxation effects and it was analyzed with a single sextet and central doublet (Fig. 4).

The spectra of A-sites showed much larger line width (Table III) compared to the B-sites and the effect being

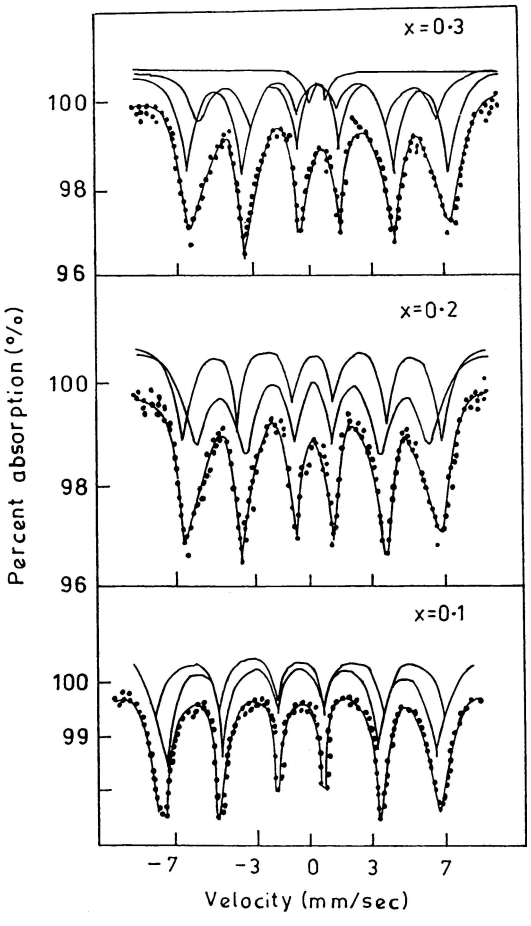

Figure 3 ^{57}Fe Mossbauer spectra at 300 K for compositions of $x = 0.1$, 0.2 and 0.3.

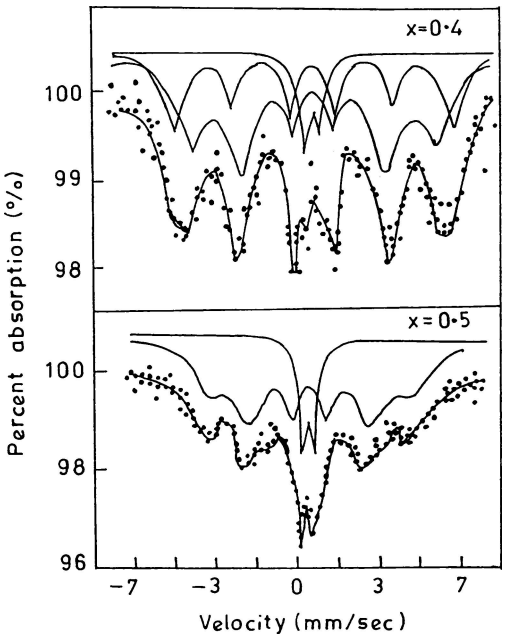

Figure 4 ^{57}Fe Mossbauer spectra at 300 K for compositions of $x = 0.4$ and 0.5.

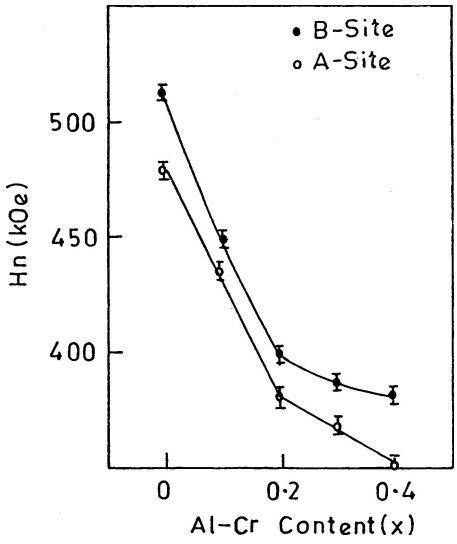

Figure 5 Variation of hyperfine fields with Al-Cr content (x).

more pronounced for $x = 0.4$. This is in conformity with the results of Belov [27]. The excessive line width of the A-sites spectrum arises because of the distribution of internal hyperfine fields. Each A-site Fe^{3+} is surrounded by 12 B-site nearest neighbours comprising magnetic Fe^{3+}, Cr^{3+}, and non-magnetic Al^{3+} ions which gives rise to the observed distribution of internal hyperfine fields at A-sites.

The iron distribution parameters $\delta = Fe_B^{3-}/Fe_A^{3+}$ deduced from the B-site to A-site Mössbauer intensity ratio (I_B/I_A) are given in Table III. The δ values found from X-ray diffraction are also given for the sake of comparison. The values of δ obtained from Mössbauer intensities are found to be about 5% higher than the δ-values obtained from X-ray data (for $x \leq 0.3$). The difference becomes awfully large for $x = 0.4$, which may be ascribed to the increase in the line widths and occurrence of the strong central paramagnetic doublet (intensity: 7.6%). Kulushreshtha [26] has observed a similar discrepancy between the Fe^{3+} Mössbauer intensity ratio and the proposed cation distribution in $NiAlFeO_4$. Moreover, the X-ray diffraction technique mainly depends upon the values of atomic scattering factors of the cations involved in the system (which are again experimentally determined) and the geometrical factors. In such circumstances, the difference about 5% in δ-values obtained from X-ray and Mössbauer data should be acceptable.

The variation of hyperfine fields (Hn) for A- and B-sites with A1-Cr concentration (x) is shown in Fig. 5. The lower value of the A-site hyperfine field compared to the B-site one is due to more covalent nature of the Fe_A^{3+}—O^{2-} bond. The variation in hyperfine fields are due to the change in A-B and B-B super transferred hyperfine interactions as the cation neighbours about a given Fe^{3+} ions are changed [28]. Since the non-magnetic Al^{3+} ions replace the magnetic Fe^{3+} ions at tetrahedral (A) sites and due to the prominent A-B super exchange interaction, the super transferred hyperfine field (H_{STHF}) at B-site is influenced to a greater extent. Therefore, initially the B-site hyperfine field decreases with a faster rate than the A-site field.

It is evident from Table III that Isomer shifts I.S (A) and I.S (B) values show very little change with Al^{3+} substitution indicating that the s-electron charge distribution of Fe^{3+} is not much influenced by Al-Cr substitution. As expected, the isomer shift of B-site Fe^{3+} ions is more positive than that for A-site Fe^{3+} because of the larger Fe^{3+}—O^{2-} bond separation in the former. No quadrupole shifts for A- and B-sites have been observed (within the experimental error) for magnetically split spectra while the central doublet observed for $x = 0.3$, 0.4 and 0.5 shows a large quadrupole splitting. This suggests that the coexistence of chemical disorder and overall cubic symmetry causes no net quadrupole shifts in Zeeman sextets; instead, it contributes to increase the line widths [29].

The observed spectra for $x = 0.3$, 0.4 and 0.5 consisted of a central doublet in addition to the broad magnetic sextet arising due to the Fe^{3+} ions presents at both the sites. The relative intensity of the central doublet was found to increase with increasing Al^{3+} concentration (Table III). The central doublet may be attributed to the Fe^{3+} ions, which are magnetically isolated and did not participate in the long range magnetic ordering due to a large number of non-magnetic nearest neighbours. For diamagnetically substituted ferrites the existence of a central doublet superimposed on well-resolved magnetic sextets has been reported for number of systems [30, 31]. In the present system the central doublet arises due to magnetically isolated Fe^{3+} ions located at the tetrahedral sites with a large number of magnetic cation as their nearest neighbours and not because of any secondary phase.

It is important to note that for other systems such as $Ni_{1-x}Zn_xFe_2O_4$ [32, 33] $Co_{1-x}Zn_xFe_2O_4$ [34, 35] $Mn_{1-x}Zn_xFe_2O_4$ [36] etc. central doublets have not been observed. The possible reason for this is that for all these systems the non-magnetic ions are at the

TABLE II Canting angle (α_β^c), magneton number (n_B) and Neel temperature (T_N) for $MgAl_xCr_xFe_{2-2x}O_4$ system

Content (x)	Canting angle $<\alpha_\beta^c>$ Degree Exp.	Theo.	n_B^M (μ_B)	RCS n_B (μ_B)	T_N (K)	T/T_N at 77 K
0.0	0	0	0.97	1.30	608	0.12
0.1	0	0	1.24	1.40	553	0.14
0.2	0	0	1.34	1.90	533	0.15
0.3	15° 17′	15° 48′	1.23	1.52	513	0.15
0.4	17° 26′	16° 57′	1.12	1.31	508	0.16
0.5	19° 33′	18° 47′	–	1.09	473	0.19
0.6	24° 17′	23° 08′	–	0.82	403	0.22
0.7	29° 09′	28° 57′	–	0.53	353	0.23
0.8	63° 50′	63° 53′	–	0.27	343	–

tetrahedral sites and some of the B-site Fe^{3+} ions should have shown the central doublet. However, each B-site Fe^{3+} ions has only six A- site ions as its nearest neighbours at a distance 0.414a (a = lattice constant) and it has other six B-site nearest neighbours at a distance of $0.353a$. This means that B-B interactions also play a significant role in addition to the A-B interaction and therefore B-site Fe^{3+} ions are not magnetically isolated and not exhibiting a central doublet. In the present system the B-site has Mg^{2+} and Al^{3+} both non-magnetic ions and the concentration of Fe^{3+} is continuously reduced. Therefore the A-site Fe^{3+} ion with many non-magnetic ions as its nearest neighbours produces the central doublet.

It is clear from Table I that the measured n_B values at 77 K exhibit a conspicuous discrepancy with the magneton numbers calculated by using Neel's theory (n_B^N) for the compositions $x \geq 0.3$. This indicates significant canting of the B-site moments, which was conjectured from the 'high field slopes', observed in M versus H curves recorded at 300 K (samples ≥ 0.3). Thus, the change of spin ordering from Neel's collinear to non-collinear type displays a strong influence on the variation of the saturation magnetic moment per molecule.

An indirect check for the presence of a canted spin structure follows from the proportionality between the nuclear hyperfine field (H_n) and the average sublattice magnetization. By neglecting intra-sublattice interactions (J_{AA}, J_{BB}) between ions on the same sites it can be shown that,

$$\mu(x) = \frac{|Hn_B(x)|}{|Hn_B(0)|} M_B(x) - \frac{|Hn_A(x)|}{|Hn_A(0)|} M_A(x)$$

where, $\mu(x)$ is the magnetic moment per formula unit, $M_B(x)$ and $M_A(x)$ are sublattice magnetizations calculated by using the free ion magnetic moments of Fe^{3+} (5 μ_B) and Cr^{3+} (3 μ_B) and the cation distribution (Equation 1). Hn_A and Hn_B are the magnitudes of the average nuclear magnetic fields for A and B-sites, respectively. Assuming that the relative saturation magnetization per formula unit $n_B(x)/n_B(0)$ at 300 K is equal to $\mu_B(x)/\mu_B(0)$, the magnetic moments per formula unit $n_B^M(x) \approx \mu(x)$ were determined from the above equation using the values of nuclear magnetic fields obtained at 300 K from the Mössbauer results. As seen from Table II, the n_B^M values agree with the n_B (observed at 300 K) for $x \leq 0.2$ while deviations it start from $x = 0.3$. This indicates that a collinear magnetic structure exists up to $x = 0.2$ and the evolution of a 'canted' spin structure begins around $x = 0.3$.

No general formula for the distribution of cations could be deduced from the X-ray and Mössbauer data analysis. Therefore, it was thought appropriate to apply the random canting model [25] instead of deriving an approximate equation based on LCS theory [37]. Since the actual spin canting depends on the number of non-magnetic nearest neighbours and their spatial arrangement, the statistical model proposed by Rosencwaig [25] should be used. According to this model, the B-site magnetic ions can be considered to be canted with an average angle $<\alpha_B>$ due to non-magnetic substitution (Al^{3+}) in A-sites which in the average nearest neighbour approximation is estimated to be,

$$\text{Cos} <\alpha_B> \sim (M_A/M_B)(J_{AB}/J_{BB})$$

The total magnetization per formula unit (i.e., magneton number) n_B^{RCS} is related to the canting angle $<\alpha_B^c>$ by

$$n_B^{RCS}(x) = M_B(x) \cos <\alpha_B^c> - M_A(x)$$

Here, M_A and M_B are sublattice magnetization of A and B-sites, respectively; and J_{AB} and J_{BB} are exchange

TABLE III Mössbauer parameters: Isomer shift (I.S.), distribution parameter ($\delta = Fe_B^{3-}/Fe_A^{3+}$), line width ($\Gamma$) and intensity of central doublet (I_d) for $MgAl_xCr_xFe_{2-2x}O_4$ system

Content (x)	I.S.(mm/s)[a] A-site	B-site	δ Mössbauer	X-ray	Γ(mm/s) A-site	B-site	Q.S.[b] (mm/sec.)	I.S. (central doublet)	I_d (%)
0.0	0.31	0.38	1.22	1.30	0.42	0.35	–	–	–
0.1	0.26	0.35	1.41	1.34	0.75	0.40	–	–	–
0.2	0.32	0.38	1.47	1.3	0.76	0.43	–	–	–
0.3	0.23	0.28	1.33	1.26	0.86	0.51	0.91	0.29	–
0.4	0.30	0.39	1.63	1.11	0.75	0.50	0.72	0.356	4.36
0.5	Relaxation I.S. = 0.36 (mm/s)		–	–	0.93		0.92	0.40	7.57

[a]With respect to iron metal, error ± 0.02 mm/s.
[b]Error: ± 0.03 mm/s.

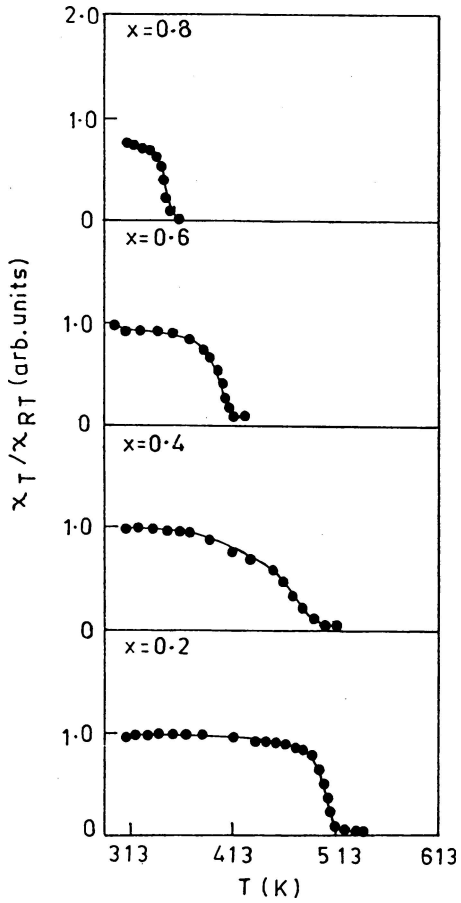

Figure 6 Thermal variation of the low field a.c. susceptibility for compositions of $x = 0.2$, 0.4, 0.6 and 0.8.

integrals. The experimental values of the canting angle $<\alpha_B^c(\text{exp})>$ have been obtained from the measured n_B values at 77 K and the same are listed in Table II. The angle of canting increases with magnetic dilution (Al-Cr content). The canting angle calculated using the RCS model is in very good agreement with the experimentally found values. It is also evident from Table I that the magneton numbers calculated using the RCS model (n_B^{RCS}) closely match with n_B (observed at 77 K). Thus, the variation of n_B as a function of Al-Cr concentration at 77 K for the system $MgAl_xCr_xFe_{2-2x}O$ can be satisfactorily explained by a random canting of spins (RCS) model.

Typical plots of the relative low field (0.5 Oe) a.c. susceptibility χ/χ_{RT} (RT = Room temperature), against temperature (T), for $x = 0.2$, 0.4, 0.6 and 0.8 are shown in Fig. 6, which exhibit normal ferrimagnetic behaviour. The Neel temperatures (T_N), determined from a.c. susceptibility measurements are listed in Table II. It is evident from Table II that there is a sharp decrease in T_N for small additions of aluminium and chromium, which is due to the decreasing number of Fe^{3+}-O^{2-}-Fe^{3+} superexchange linkages resulting from replacement of Fe^{3+} by Al^{3+}-Cr^{3+} in the spinel lattice.

4. Conclusions

The lattice constant 'a' decreases linearly with Al-Cr content at different rates which is due to the inter-play of Al^{3+} and Fe^{3+} cations on A- and B-sites. There is a good agreement between the cation distribution deduced from X-ray diffraction and from Mössbauer spectroscopic measurements. The Mössbauer spectra at 300 K exhibit two Zeeman sextets and can be analyzed with a single sextet and a central doublet. The spectra for $x = 0.3$ and 0.4 show the presence of a central paramagnetic doublet superimposed on two sextets and its intensity increases with Al-Cr content. The central doublet is ascribed to magnetically isolated Fe^{3+} ions. The substitution of Al^{3+} causes an excessive increase in the line width of the Mössbauer spectra, particularly for the A-site spectrum. The variation of magneton number can be successfully explained by invoking the Random Canting of spins (RCS) model. Thermal variation of the a.c. susceptibility exhibits normal ferrimagnetic characteristics.

Acknowledgements

One of the authors (KBM) is thankful to AICTE, New Delhi for providing financial assistance in the form of career award for young teachers.

References

1. H. KNOCK and H. DANNHEIM, *Phys. Stat. Solid.* A**37** (1976) K235.
2. E. DE GRAVE, C. DAUVE, A. GOVARERT and J. D. SILLER, *ibid.* B**78** (1967) 527.
3. A. B. BALDEV, O. A. BAYUKOV and A. F. SAVITSKI, *ibid.* **152**(5) (1989) 639.
4. U. SCHMOCAER, H. R. BOESCH and F. WAIDNER, *Phys. Lett.* **40A** (1972) 237.
5. K. B. MODI, N. N. JANI and H. H. JOSHI, *Ind. J. Pure Appl. Phys.* **33** (1995) 758.
6. K. B. MODI, H. H. JOSHI and R. G. KULKARNI, *J. Mater. Sci.* **31** (1996) 1311.
7. KUNAL B. MODI and H. H. JOSHI, *J. Mater. Sci. Lett.* **17** (1998) 741.
8. S. J. SHUKLA, K. M. JADHAV and G. K. BICHILE, *Ind. J. Pure Appl. Phys.* **39** (2001) 226.
9. U. N. TRIVEDI, K. B. MODI and H. H. JOSHI, *Pramana J. Phys.* **58** (2002) 1031.
10. U. N. TRIVEDI, K. B. MODI, D. C. KUNDALIYA, A. G. JOSHI, H. H. JOSHI and S. K. MALIK, "VI Latin American Workshop on Magnetism" (Magnetic Materials and Their Applications, Mexico, 2003).
11. URVI V. CHHAYA and R. G. KULKARNI, *Matt. Lett.* **39** (1999) 91.
12. U. V. CHHAYA, B. S. TRIVEDI and R. G. KULKARNI, *Physica B* **262** (1999) 5; *Hyperf. Interact.* **116** (1998) 197.
13. K. H. JANI, Ph.D. Thesis, Saurashtra University, Gujarat, India, 2002.
14. V. D. MURUMKAR, K. B. MODI, K. M. JADHAV, G. K. BICHILE and R. G. KULKARNI, *Matt. Lett.* **32** (1997) 28.
15. C. R. K. MURTHY, S. D. LIKHITE and N. P. SHASTRY, *Philos. Magl.* **23** (1971) 503.
16. C. R. K. MURTHY, S. D. LIKHITE and P. SAHASRABUDHE, *Proc. Ind. Acad. Sci.* **87A** (1978) 245.
17. B. D. CULLITY, "Elements of X-ray Diffraction" (Addison-Wesley Pub. Co., 1978).
18. M. J. BUERGER, "J. Crystal Structure Analysis" (John-Wiely, New York, 1960).
19. C. G. WHINFREY, D. W. ECKORT and A. TAUBER, *J. Am. Chem. Soc.* **53** (1982) 2722.
20. S. K. KULUSHRESHTHA and G. RITTER, *J. Mater. Sci.* **20** (1985) 821.

21. M. D. SUNDARAJAN, A. NARAYANASAMY, T. NAGARAJAN, L. HAGGSTRON, C. S. SWAMY and K. V. RAMANUJACHARY, *J. Phys. C. Solid State Phys.* **17** (1984) 2453.
22. L. NEEL, *Ann. Phys.* **3** (1948) 137.
23. B. D.CULLITY, "Introduction to Magnetic Materials" (Addison-Wesley Pub. Co., 1972).
24. S. K. KULUSHRESHTHA, *J. Mater. Sci.* **5** (1986) 638.
25. A. ROSENCWAIG, *Can. J. Phys.* **48** (1970) 2857.
26. S. K. KULUSHRESHTHA, *J. Mater. Sci.* **5** (1986) 638.
27. V. F. BELOV, M. N. SCHIPLCO, T. A. KHIMICH, V. V. KOROVUSHKINA and L. N. KUBROLIN, *Sov. Phys. Solid State Phys. (Eng. Trans.)* **13** (1971) 1672.
28. F. VAN DER WOUDE and G. A. SAWATZKY, *Phy. Rev. B* **4** (1971) 29.
29. H. H. JOSHI and R. G. KULKARNI, *Solid State Commun.* **60** (1986) 67.
30. E. DE GRAVE, D. CHAMBAERE and G. ROBBERRECHT, *J. Mag. Mag. Mater.* **15** (1980) 643.
31. E. DE GRAVE, R. VANLEERBERGHE, G. DAUWE, A. GOVAERT and J. DE SITTER, *J. de. Phys.* **37** (1976) 97.
32. S. C. BHARGAVA and N. ZEEMAN, *Phys. Rev. B* **21** (1980) 1726.
33. *Idem.*, *ibid.* **21** (1980) 1717.
34. S. C. BHARGAVA and P. K. IYENGAR, *Phys. Status Solid. (B)* **46** (1971) 117.
35. *Idem., ibid.* **53** (1972) 352.
36. D. E. COX, G. SHIRANE, P. A. FLINM, S. L. RUBY and W. J. TAKAI, *Phys. Rev.* **132** (1963) 1547.

Received 4 March 2003
and accepted 14 October 2004